ACS OMEGA

http://pubs.acs.org/journal/acsodf

Article

Experimental and Theoretical Study on the Gas-Phase Reactions of Germyl Radicals with NF_3: Homolytic Substitution at the Nitrogen Atom vs Fluorine Abstraction

Paola Antoniotti,* Paola Benzi, Domenica Marabello, and Daniele Rosso

Cite This: *ACS Omega* 2020, 5, 4907−4914

Read Online

ACCESS | Metrics & More | Article Recommendations | Supporting Information

ABSTRACT: In this paper, we report on the unexplored reaction mechanisms of bimolecular homolytic substitution (S_H2) between GeH_3 radicals and the nitrogen atom of NF_3. The S_H2 reactions are studied both experimentally and theoretically with ab initio and density functional theory (DFT) calculations. The experimental results of X-ray irradiation of mixtures of GeH_4 and NF_3 show the formation of GeH_3−NF_2 and GeH_3−F. The trend of product yields as a function of the increase in GeH_4 partial pressure in the irradiated mixtures evidences the predominant role of GeH_3 radicals. Particularly, the S_H2 mechanism can be hypothesized for the reaction between GeH_3 radicals and NF_3 molecules leading to GeH_3−NF_2. This mechanism is further confirmed by the increase in GeH_3−NF_2 yield observed if O_2 is added, as a radical scavenger, to the reaction mixture. In agreement with the experimental data, from the calculations performed at the CCSD(T) and G3B3 levels of theory, we observe that the GeH_3−NF_2 product actually occurs from a bimolecular homolytic substitution by the GeH_3 radical, which attacks the N atom of NF_3, and this reaction is in competition with the fluorine abstraction reaction leading to GeH_3F, even if other mechanisms may be involved in the formation of this product.

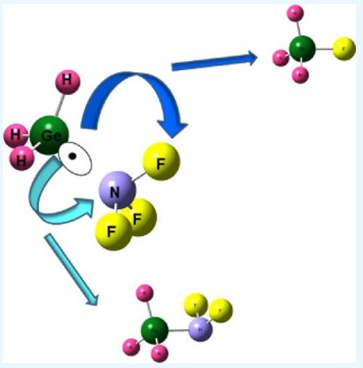

INTRODUCTION

Bimolecular homolytic substitution (S_H2) reactions are classical reactions of free radicals, following reaction 1

$$R_1 + Y - R_2 \; Y - R_1 + R_2 \qquad (1)$$

Over the years, the S_H2 reactions (reaction 1) have received considerable attention both from experimental and theoretical points of view. In fact, they are elementary steps of many chemical reactions, are observed with different types of radicals (R_1), and can be useful not only in the development of novel synthetic methodologies, particularly to generate new radicals, but also for the formation of carbon−carbon and carbon−heteroatom bonds (C−S, C−Si, C−Se, C−Sn, and so forth).[1]

Generally, these reactions occur at the univalent hydrogen or halogen atoms (Y = H, Cl, Br, I) but mostly proceed at the main-group heteroatoms (Y = Si, Ge, Sn, P, O, S, and Se, Te).[2]

It is generally recognized that the S_H2 reactions occur with a backside mechanism, in which the attack of R_1 and the expulsion of R_2 (in reaction 1) occur in opposite directions and involve a collinear (or nearly collinear) transition structure (TS) or a hypervalent intermediate.[3−5] A frontside R_1 attack has also been proposed, and the two mechanisms can be in competition.

Both of the mentioned mechanisms can occur for the homolytic substitution of methyl and acetyl radicals at disilane, digermane, distannane, silylgermane, silylstannane, and germylstannane.[6] Recently, the reaction of phenyl radicals with silane was studied both experimentally and theoretically to investigate the chemical dynamics of phenylsilane formation via bimolecular radical substitution.[7] The occurrence of frontside and backside mechanisms in the homolytic substitution by silyl, germyl, and stannyl radicals at the heteroatom in disilane, digermane, distannane, silylgermane, silylstannane, and germylstannane has also been theoretically investigated by Schiesser and co-workers.[8] Processes like these were first reported by Cadman et al.,[9] and more recently, Belter[10] explored the reactivity of NF_3 with aliphatic and aromatic substrates. However, despite the general interest in this kind of reaction, there is a lack of information about the S_H2 reaction between radicals and nitrogen-containing molecules.

In our previous work, we investigated the reactions between NF_3 and the radicals CH_3, C_2H_5, and *i*-C_3H_7, generated by X-ray irradiation of the corresponding iodides R-I, and we performed ab initio and density functional theory (DFT) calculations on the observed reactions. The results of our investigation indicate that R-NF_2 is obtained from a S_H2 reaction by the alkyl radicals R, which attack the N atom of

Received: November 4, 2019
Accepted: January 15, 2020
Published: March 3, 2020

https://dx.doi.org/10.1021/acsomega.9b03729
ACS Omega 2020, 5, 4907−4914

Table 1. Mean Energy Absorbed to Form an Ion Pair W (J molecule^{-1}), Ionization Potential I (J molecule^{-1}), and Energy (ΔE) Values Related to Reactions 2−4[a,b]

W	I	W − I	ΔE	radicals per ion
5.18×10^{-18}	$2{,}16 \times 10^{-18}$	3.02×10^{-18}	4.03×10^{-19}	7.5
4.03×10^{-18}	1.68×10^{-18}	2.35×10^{-18}	5.96×10^{-19}	3.9
4.03×10^{-18}	1.68×10^{-18}	2.35×10^{-18}	3.68×10^{-19}	6.4

[a]The calculated number of radicals for each formed ion is also shown. [b]The experimental values of W for NF_3 and GeH_4 are not available, but it is known that for gaseous molecules the ratio W/I ranges from 2.2 to 2.6.[23] Thus, W was obtained from the average value of W/I and the ionization potential of NF_3[16] and GeH_4.[24]

Table 2. Average Empirical Formula and Hydrogenation Degree (H/(Ge + N) Atomic Ratio) of the Solids Obtained by X-ray Irradiation, with 100 kGy, of the GeH_4/NF_3 Mixtures with Different Compositions

NF_3 percentage	30%	50%	70%
empirical formula	$Ge_{4.35}N_1F_{1.676}H_{7.47}$	$Ge_{3.77}N_1F_{1.45}H_{6.31}$	$Ge_{3.29}N_1F_{1.57}H_{5.06}$
H/(Ge + N) atomic ratio	1.40	1.32	1.18

NF_3, while the attack of alkyl radicals at the F atom(s) of NF_3[11] leads to R-F products.

In this work, following our interest in the gas-phase reactions between the fluorinated compounds and hydrides of C, Si, and Ge,[12] we decided to further investigate the S_H2 reactions at the nitrogen atom using NF_3 as a substrate. In particular, taking into account that the homolytic bimolecular substitution mechanism that occurs at the nitrogen atom by means of the germyl radical is still not explored, we studied the reactions between GeH_3 radicals generated by X-ray irradiation and NF_3. For this purpose, we used a combined approach involving long-time static X-ray radiolysis, gas chromatography−mass spectrometry analysis at very low temperatures, and high-level theoretical calculations. We irradiated mixtures of GeH_4/NF_3 at several partial pressures of reagents, with different irradiation doses. Moreover, we also used an effective Ge and GeH_2 radical scavenger to highlight the reactions of the GeH_3 radicals. Three different levels of theory (CASSCF, CCST(T), and G3B3) have been used to verify the expected reaction mechanisms between the GeH_3 radicals and the NF_3 molecules.

RESULTS AND DISCUSSION

Radiolysis of GeH_4/NF_3 Mixtures. X-ray irradiation of GeH_4/NF_3 mixtures can produce both ionic and radical species that lead to the formation of new gaseous species and to the deposition of solid products.

The relative contribution of radicals and ions to the formed products can be evaluated considering the average energy absorbed to form the ion pair, W (i.e., the energy related to the process: $M \rightarrow M^+ + e^-$; M = GeH_4 or NF_3), and the ionization energy, I.[13,14] The difference between W and I is always positive, and the W − I excess energy is available to form excited molecules and/or radicals.

During the radiolysis of pure NF_3, the following radicals are produced, according to the dissociation reaction:

$$NF_3 \rightarrow NF_2 + F \quad (2)$$

The primary radicals formed during the radiolysis of pure GeH_4 are germyl (GeH_3) and germylene (GeH_2) radicals; it has been proposed[15] that their formation occurs by decomposition of excited molecules according to eqs 3 and 4

$$GeH_4 \rightarrow GeH_3 + H \quad (3)$$

$$GeH_4 \rightarrow GeH_2 + H_2 \quad (4)$$

The activation energy required for the formation of GeH_3 and GeH_2 radicals is 355.6 and 221.8 kJ mol^{-1}, respectively; thus, the reaction forming GeH_2 radicals is favored.[16] Moreover, it was also observed that GeH_2 is further decomposed to give Ge and GeH and the corresponding reactions compete with each other in the ratio 9:1.[15]

The W and I values of NF_3 and GeH_4 are listed in Table 1, together with the energy values related to reactions 2−4.[16]

From these data, it is possible to evaluate the radicals formed for each ion: about seven from NF_3 and about four or six from GeH_4 if reactions 3 and 4 are considered, respectively. Therefore, the observed products obtained from radiolysis can be considered to be mainly due to radical reactions.

Moreover, the total energy absorbed by the mixture is related to the irradiation dose (Gy = J Kg^{-1}), and it is shared between GeH_4 and NF_3 on the basis of their mass. Therefore, even if it is not possible to calculate the actual yields of the GeH_3 and GeH_2 primary radicals, it is reasonable to suppose that the total energy absorbed by germane is split in reactions 3 and 4 with the same ratio in all mixtures, and hence, the GeH_3/GeH_2 radical ratio is constant.

All radicals formed participate in the reactions leading to solid and gaseous products, but the results of our previous works obtained from theoretical calculations, mass spectrometry, and radiolysis on mixtures containing germane with and without oxygen indicate that the radicals involved in the deposition of the solid product are different from the radical precursors of primary gaseous species detected after radiolysis experiments.[15,17] In particular, the hydrogen-poor species from germane (GeH_2 and Ge radicals and ions) are involved in the polymerization processes leading to solid products but not in those leading to primary gaseous products. In fact, if O_2 is added as a radical scavenger (which reacts with GeH_2 but not with GeH_3), an oxygenated solid product is obtained, whereas no variation in gaseous product yields is observed.[15,17] This fact also indicates that the GeH_3 (radicals and ions) can be considered to be related to the formation of the observed primary gaseous species.[15,17] On the other hand, in a previous work on ion−molecule reactions occurring in the GeH_4/NF_3gaseous mixture investigated by ion trap mass spectrometry and ab initio calculations,[12b] we observed that the GeH_3^+ ion does not react with NF_3 and no ionic products with Ge−N connectivity[12b,c] were evidenced. Therefore, it is reasonable to suppose that the primary gaseous species observed after radiolysis are attributable to reactions involving GeH_3 radicals.

https://dx.doi.org/10.1021/acsomega.9b03729
ACS Omega 2020, 5, 4907−4914

Table 3. μ-Moles of GeH_3NF_2 and GeH_3F Obtained from X-ray Irradiation of GeH_4/NF_3 Mixtures for Different GeH_4/NF_3 Partial Pressures and for Different Irradiation Doses[a]

	GeH_4/NF_3					
mixture (Torr)	490/210		350/350		210/490	
dose (kGy)	100	200	100	200	100	200
GeH_3F	97.0	143.0	62.0	105.0	34.0	88.0
GeH_3NF_2	20.2	23.0	18.0	18.0	13.0	19.0
GeH_3F/GeH_3NF_2	4.8	6.22	3.44	5.83	2.62	4.63

[a] μ-mole determinations are affected by errors of about ±15%; 1.0 Torr = 1.91×10^{-2} mmol.

The characterization of solids obtained from irradiation of the GeH_4/NF_3 mixtures indicates that they are networked polymers of Ge and N, with dangling bonds saturated with F and H atoms. The average empirical formula (obtained by elemental and X-ray photoelectron spectroscopy (XPS) analysis) and hydrogenation degree (H/(Ge + N) atomic ratio) of the solids obtained by X-ray irradiation (100 kGy) of the GeH_4/NF_3 mixtures with different compositions are reported in Table 2.

The low values of the hydrogenation degree of solids, varying between 1.40 and 1.18 when GeH_4 ranges from 70 to 30%, suggest that even in the GeH_4/NF_3 mixtures the hydrogen-poor active species (principally radicals) of germane play a predominant role in the reaction pattern, leading to the condensed phase and confirming the above-reported hypothesis.

The gas chromatography−mass spectrometry (GC−MS) analysis of the gas phase after irradiation of GeH_4/NF_3 mixtures shows that GeH_3F forms in an appreciable quantity and GeH_3NF_2 in smaller quantities. Other products are also observed: a fair amount of digermane and a small amount of HNF_2. The product yields detected from experiments performed with two different irradiation doses (100 and 200 kGy) and with different GeH_4/NF_3 relative pressures are shown in Table 3.

From Table 3, it is observed that the yields of GeH_3F and GeH_3NF_2 in the gas phase increase if the GeH_4 relative pressure in the irradiated mixture is increased, suggesting that even for GeH_4/NF_3 mixtures the reactions leading to gaseous products happen through mechanisms that involve germyl radicals and NF_3 molecules. This process contributes only in part to the GeH_3F product, and other processes must be considered; for example, the substitution reaction of F radicals that replace the hydrogen of GeH_4. In fact, the ratio between the GeH_3F and GeH_3NF_2 product yields decreases if the NF_3 percentage in the mixture is increased, suggesting that the F radicals produced by X-ray fragmentation of NF_3 contribute to the formation of the GeH_3F product. Nevertheless, the finding that the GeH_3F yield decreases significantly even if NF_3 increases from 30 to 70% (and hence F radicals are increased by a factor of 2.3) indicates that the F radicals contribute to the total GeH_3F amount only to a minor extent.

Table 4 reports the results of GC−MS analysis of the gas phase after irradiation of the GeH_4/NF_3 mixtures with different partial pressures of GeH_4 (600 and 400 Torr) and a constant partial pressure of NF_3 (400 Torr). Table 4 also reports the results obtained by adding O_2 as a radical scavenger.

The results of Table 4 show a sharp decrease in both GeH_3F and GeH_3NF_2 products with decreasing GeH_4 partial pressure but a constant partial pressure of NF_3 (400 Torr) and, hence, with the expected same amount of F radicals. This fact evidences the predominant role of GeH_3, confirming the above hypothesis.

Table 4. μ-Moles of GeH_3NF_2 and GeH_3F Obtained from X-ray Irradiation of GeH_4/NF_3 Mixtures with a NF_3 Pressure of 400 Torr and Different GeH_4 Partial Pressures, with an Irradiation Dose of 10 kGy[a,b]

	GeH_4/NF_3		$GeH_4/NF_3 + O_2$
mixture (Torr)	600/400	400/400	600/400/100
GeH_3F	11.9	6.25	40
GeH_3NF_2	5.52	3.52	25
GeH_3F/GeH_3NF_2	2.2	1.8	1.6

[a] The results obtained by adding O_2 as a radical scavenger are also shown. [b] μ-mole determinations are affected by errors of about ±15%; 1.0 Torr = 1.91×10^{-2} mmol.

Table 3 also shows the variations of GeH_3F and GeH_3NF_2 yields with different irradiation doses. To explain these results, it must be considered that the new products formed by irradiation modify the mixture composition and can participate in the reaction as both molecular and radical/ionic species. Thus, the observed yields are a result of the competition between formation and decomposition reactions, and they can vary with doses in a not easily predictable way. Nevertheless, from Table 3, some qualitative considerations can be made: (i) the GeH_3F and GeH_3NF_2 yields increase with dose for all mixtures (except for GeH_3NF_2 in the 50% mixture), indicating that the formation reaction always prevails over the decomposition one and suggesting the high stability of these species even under the radiolysis condition; (ii) the sharp increase in GeH_3F with dose indicates the rather high reactivity of GeH_3 radicals toward NF_3; (iii) the yield increment of the gaseous products is higher if the NF_3 percentage in the mixture increases: variations from 47 to 160% and from 14 to 46% for GeH_3F and GeH_3NF_2 are observed, respectively, if the NF_3 pressure is varied from 30 to 70%. This confirms the above-reported hypothesis that the GeH_2 radicals play a predominant role in the polymerization process, leading to solid deposition, while the GeH_3 radicals are involved in the reaction mechanisms of the gaseous product formation.

In fact, even the products of radiolysis, such as GeH_3F and GeH_3NF_2, can react with GeH_2 radicals in the radical polymerization reactions leading to solid products; for example

$$GeH_3NF_2 + GeH_2 \rightarrow Ge_2NF_xH_y + H \text{ or } F \ (x = 1, 2; y = 4, 5) \quad (5)$$

$$GeH_3F + GeH_2 \rightarrow Ge_2NF_xH_y + H \text{ or } F \ (x = 1, 0; y = 4, 5) \quad (6)$$

https://dx.doi.org/10.1021/acsomega.9b03729
ACS Omega 2020, 5, 4907−4914

The lower amount of GeH_2 radicals in the higher NF_3 percentage mixture makes reactions 5 and 6 less probable, favoring the increase in the yields of GeH_3F and GeH_3NF_2.

The same effect is obtained if O_2 is used as a radical scavenger (Table 4). In fact, oxygen effectively scavenges the GeH_2 radicals but not the GeH_3 radicals,[15,17] leading to oxygenated solid products, thus decreasing the extent of reactions 5 and 6 and increasing the GeH_3F and GeH_3NF_2 yields.

COMPUTATIONAL RESULTS

The experimental results suggest that both products GeH_3-NF_2 and GeH_3-F can be obtained by competitive reactions of the GeH_3 radicals with NF_3. The GeH_3-NF_2 product can arise from the bimolecular homolytic substitution (reaction 7), occurring at the nitrogen atom of NF_3, while the GeH_3-F product can be considered to be mainly due to the F-atom abstraction reaction (reaction 8) through the attack of GeH_3 on the F atom(s) of NF_3, even if other reaction mechanisms can contribute to this product yield.

$$GeH_3 + NF_3 \rightarrow GeH_3 - NF_2 + F \quad (7)$$

$$GeH_3 + NF_3 \rightarrow GeH_3 - F + NF_2 \quad (8)$$

To confirm the experimental results and the predicted reaction mechanisms, a theoretical study of the potential energy surface related to the reactions of GeH_3 with NF_3 was carried out.

The geometries of intermediates and TS_S (Figures 1 and 2) were optimized with three different theoretical models: a multideterminantal CASSCF model in conjunction with the 6-31G(d) basis set, perturbative MP2(full) and DFT/B3LYP methods, which include the electron correlation with the 6-311G(d,p) basis set.

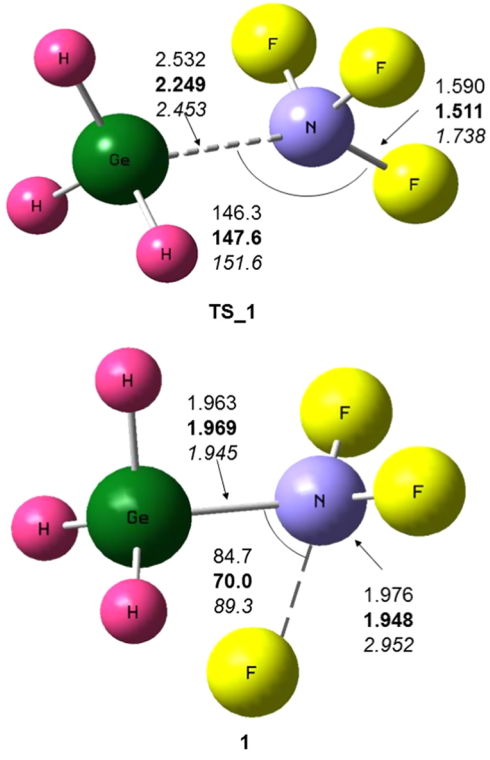

Figure 1. CASSCF(9,6)/6-31G(d) (italics), MP2(full)/6-311G(d,p) (bold), and B3LYP/6-311G(d,p) optimized geometries (angstrom and degree) of the species involved in the S_H2 reaction between GeH_3 and NF_3.

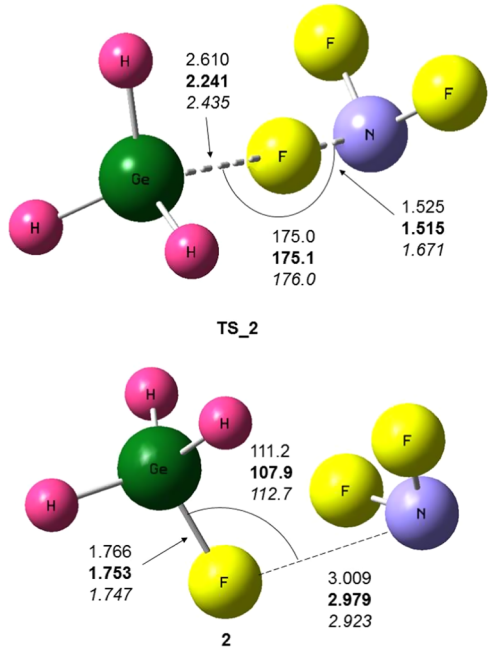

Figure 2. CASSCF(9,6)/6-31G(d) (italics), MP2(full)/6-311G(d,p) (bold), and B3LYP/6-311G(d,p) optimized geometries (angstrom and degree) of the species involved in the F extraction reaction between GeH_3 and NF_3.

The corresponding potential enthalpy diagram obtained at the CCSD(T,full)/6-311++G(2d,2p)//CASSCF(9,6)/6-31G(d) level of theory is reported in Figure 3. The energy (ΔE), enthalpy (ΔH), and free energy (ΔG) differences of the various species, computed at the CCSD(T,full)/6-311++G-(2d,2p)//CASSCF(9,6)/6-31G(d), CCSD(T,full)/6-311++G(2d,2p)//MP2(full)//6-311G(d,p), and G3B3 levels of theory, are listed in Table 5.

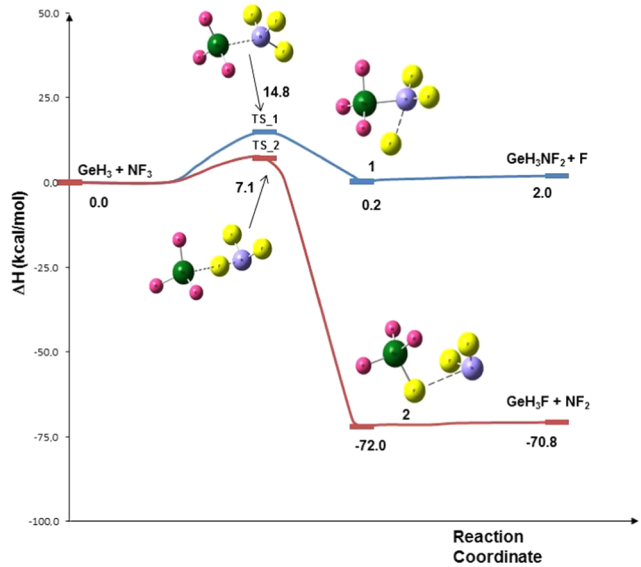

Figure 3. CCSD(T,full)/6-311++G(2d,2p)//CASSCF(9,6)/6-31G(d) relative enthalpies at 298.15 K (kcal mol^{-1}) of the species involved in the reactions between GeH_3 and NF_3.

https://dx.doi.org/10.1021/acsomega.9b03729
ACS Omega 2020, 5, 4907−4914

Table 5. Relative Energies ΔE at 0 K [kcal mol^{-1}], Relative Enthalpies ΔH at 298.15 K [kcal mol^{-1}], and Relative Free Energies ΔG at 298.15 K [kcal mol^{-1}] of the Species Involved in the Reactions between GeH_3 and NF_3

	CCSD(T,full)/6-311++G(2d,2p)[a]			CCSD(T,full)/6-311++G(d,p)[b]			G3B3[c]		
species	ΔE	ΔH	ΔG	ΔE	ΔH	ΔG	ΔE	ΔH	ΔG
GeH_3 + NF_3	0.0	0.0	0.0	0.0	0.0	0.0	0.0	0.0	0.0
TS_1	14.7	14.8	24.1	18.8	18.7	29.4	14.7	14.8	24.1
TS_2	7.1	7.1	14.3	11.1	11.0	21.1	7.2	7.1	21.8
1	0.0	0.2	8.5	−6.2	−6.3	3.7	−0.8	−0.1	5.4
2	−72.0	−72.0	−64.8	−71.7	−70.9	−63.8	−69.7	−69.1	−62.7
GeH_3NF_2 + F	1.8	2.0	15.7	1.8	1.4	15.0	6.4	6.7	9.3
GeH_3F + NF_2	−70.8	−70.8	−71.0	−69.9	−69.7	−69.2	−67.8	−67.9	−68.1

[a]At the CASSCF/6-31G(d) optimized geometries. [b]At the MP2(full)/6-311G(d,p) optimized geometries. [c]At the B3LYP/6-311G(d,p) optimized geometries.

Several previously published studies[18−22] show that NF_3 acts as a Lewis base that interacts with electrophilic species through the N and F atoms. Therefore, we explored the attack of GeH_3 on both atoms, and located the energy minima **1** and **2** and the transition states **TS_1** and **TS_2** shown in Figures 1 and 2. These minima and TSs are connected as shown in Figure 3. An intermediate **1′** is also formed before reaching the transition states **TS_1** and **TS_2**, but it is thermochemically and thermodynamically unstable at all levels of calculation (see Figure S1 and Table S4).

The interaction between the GeH_3 radical and the N atom of NF_3 leads to transition state **TS_1** and takes place through the homolytic substitution of GeH_3 at the N atom of NF_3 with elimination of an F atom. **TS_1** shows a rather long Ge−N bond, as typically occurs in this mechanism, corresponding to 2.453, 2.532, and 2.249 Å at the CASSCF, B3LYP, and MP2(full) levels, respectively. The N−F bond is 1.738, 1.590, and 1.511 Å at the CASSCF, B3LYP, and MP2(full) levels of theory, respectively. The Ge−N−F angle is 151.6° at the CASSCF level, compared to 146.3 and 147.6° calculated at the B3LYP and MP2(full) levels of theory, respectively.

The intrinsic reaction coordinate (IRC) calculations show that **TS_1** connects the reactants with the weakly bound molecular complex **1** (see Figure 1). In intermediate **1**, an F atom is rather distant from the N atom of GeH_3NF_2 and the N−F bond length and the Ge−N−F bond angle depend on the computational level. In particular, it progressively reduces from the CASSCF (2.952 Å, 89.3°) to the B3LYP (1.976 Å, 84.7°) and the MP2(full) (1.948 Å, 70.0°) levels.

The analysis of the occupation of the active space orbitals of intermediate **1** shows the presence of a doubly occupied σ_{NF} bond orbital and a singly occupied σ^*_{NF} antibonding orbital. This electronic configuration together with the long bond distance and the low dissociation energy allows us to classify this as a 2c−3e bond.

The interaction between the GeH_3 radical and the F atoms of NF_3 leads to transition state **TS_2**, which adopts an almost linear arrangement of the GeH_3 radical and NF_2 at any computational level, in agreement with the previously studied reactions of alkyl radicals with NF_3.[11] The Ge−F bond distance increases, according to the calculation level used, from 2.241 to 2.435 and to 2.610 Å at the MP2(full), CASSCF, and B3LYP levels of theory, respectively. At the MP2(full) and B3LYP levels of theory, the N−F bond lengths are comparable and amount to 1.515 and 1.525 Å, respectively. Instead, the CASSCF level furnishes a greater bond distance of 1.671 Å. The intrinsic reaction coordinate (IRC) calculations show that **TS_2** does not connect the reactants to the products, but to the weakly bound complex **2** (see Figure 2). Complex **2** results from the interaction of the F atom of GeH_3F with the N atom of NF_2, as shown by the long N−F bond distance which is 2.923, 2.979, and 3.009 Å, at the CASSCF, MP2(full), and B3LYP levels of theory, respectively. The analysis of the occupation of the active space orbitals of intermediate **2** does not allow classifying the interaction between the two fragments as a 2c−3e bond.

The T1 diagnostics of **TS_1** (0.028) and **TS_2** (0.025) are slightly higher than the accepted threshold of 0.020, for a monodeterminantal wave function. However, the CI coefficients of the ground-state CASSCF wave function are 0.94 and 0.95 for **TS_1** and **TS_2**, respectively. This indicates that the greatest weight is given by the ground-state configuration and also suggests the prevailing role of dynamic correlation, allowing the use of a monodeterminant theoretical model such as the G3B3.

The S_H2 reaction 7, passing through **TS_1**, shows an enthalpy barrier of 14.8 kcal mol^{-1} at the CCSD(T)//CASSCF and 18.7 kcal mol^{-1} at the CCSD(T)//MP2(full) level, and the F-atom abstraction (reaction 8), passing through **TS_2**, shows an enthalpy barrier of 7.1 kcal mol^{-1} at the CCSD(T)//CASSCF and 11.0 kcal mol^{-1} at the CCSD(T)//MP2(full) level. The two enthalpy barriers of reactions 7 and 8, at the G3B3 level, correspond to 14.8 and 7.1 kcal mol^{-1} and coincide surprisingly with the results obtained at the CCSD(T)//CAS level of theory (Table 5). The small enthalpy difference between the two barriers allows a competition between the reactions.

The dissociation of complex **1** into the products needs to overcome an enthalpy barrier of nearly 2 kcal mol^{-1} at the CCSD(T)//CAS level of theory, which becomes slightly higher at the CCSD(T)//MP2(full) (7.7 kcal mol^{-1}) and G3B3 levels of theory (6.8 kcal mol^{-1}). Complex **2** dissociates into fragments GeH_3F and NF_2 through a barrier of 1.2 kcal mol^{-1} at all computational levels.

The already known reaction 7 of fluorine atom abstraction by germyl radicals is exothermic by 66.9 kcal mol^{-1}, from experimental data.[16,23] This result is consistent with our theoretical calculations, which provide for reaction 7 an exothermicity of 70.8, 69.7, and 67.9 kcal mol^{-1} at the CCSD(T)//CAS, CCSD(T)//MP2(full), and G3B3 levels of theory, respectively.

CONCLUSIONS

In this work, we report on the unexplored homolytic bimolecular substitution mechanism that occurs at the nitrogen atom by means of a germyl radical. In fact, the experimental

https://dx.doi.org/10.1021/acsomega.9b03729
ACS Omega 2020, 5, 4907−4914

and computational results indicate that the S_H2 mechanism effectively occurs, leading to GeH_3NF_2, and it is in competition with the fluorine abstraction reaction, leading to GeH_3F.

The computational results have shown that the energy barriers of the S_H2 reaction 7 (about 15−19 kcal mol^{-1}) and of the fluorine abstraction (8) (about 7−9 kcal mol^{-1}) are slightly different, taking into account that the energies, obtained at different levels of calculation, are affected by an uncertainty of about ±2−4 kcal mol^{-1}. The enthalpy of these two processes is instead very different. Reaction 8 is strongly exothermic by 68−71 kcal mol^{-1}, and this result is in excellent agreement with the experimental result of about 67 kcal mol^{-1} in the literature. Instead, reaction 7 is slightly endothermic at all levels of calculation. Both the energy barriers and the enthalpy of reactions are in good agreement with the yield of the products obtained from the experiments. In fact, we have observed the formation of an appreciable amount of GeH_3F from the strongly exothermic reaction 8, with a lower energy barrier, and a minor amount of GeH_3NF_2 from the slightly endothermic reaction 7, with a higher energy barrier. Furthermore, the finding that the yields of the two reactions increase as a function of both the partial pressure of GeH_4 and the irradiation dose and that the same result is obtained after adding O_2 as a radical scavenger, which effectively reacts with Ge and GeH_2 but not with GeH_3, confirms the predominant role of the germyl radicals in the formation of both products.

EXPERIMENTAL METHODS

Materials. Caution: The preparation and manipulation of gaseous NF_3 and GeH_4 and their mixtures require precaution because explosive products can be formed.

NF_3 at 99.99% stated purity and GeH_4 and pure O_2 were supplied by Praxair. GeH_4 was purified by bulb-to-bulb distillation under vacuum and dried with sodium sulfate before use. The GeH_4/NF_3 mixtures were prepared in 350 mL Pyrex vessels. Standard vacuum techniques were used to handle reactants and gaseous products.

X-ray Radiolysis. Mixtures of GeH_4 + NF_3 with different compositions at a total pressure of 700 Torr were irradiated at absorbed irradiation doses of 100 and 200 kGy. GeH_4/NF_3 mixtures with an NF_3 pressure of 400 Torr and different GeH_4 partial pressures [600 and 400 Torr] and with O_2 as a radical scavenger were also irradiated with an irradiation dose of 10 kGy.

A CPXT-320 tube (GILARDONI) with a maximum output of 320 keV was used as the X-ray source for irradiation at 100 and 200 kGy doses. An Eresco 160 MF4-R with a maximum output of 160 keV was used for irradiation at 10 kGy.

Gas Chromatography−Mass Spectrometry Analysis. After irradiation, a small amount of the gaseous phase was collected for qualitative and quantitative analyses of volatile compounds by GC−MS. A Varian 3400/ Finnigan ITD instrument was employed, equipped with an Alltech AT-1 capillary column (polydimethylsiloxane, 30 m long, 0.25 mm internal diameter, 1.0 mm film thickness). Before injection, the GC oven was cooled at 193 K by introducing liquid nitrogen; afterward, the column was heated up to 433 K with the following temperature program: isothermal starting step at 193 K for 4 minutes; heating step up to 373 K (20 K min^{-1}); isothermal step at 373 K for 10 minutes; heating step up to 433 K (30 K min^{-1}); isothermal step at 433 K for 3 minutes; cooling step to room temperature. A split of about 16 mL min^{-1} was applied during injection; helium was used as the carrier gas at a flow rate of 0.8 mL min^{-1}. Electron ionization was performed at 70 eV, and the spectra were collected in the 15−500 u mass range.

Computational Methods. The calculations were performed with the GAUSSIAN09[25] program. The geometries of the reagents, intermediates, products, and transition states (TSs) involved in the reactions between the GeH_3 radicals and NF_3 were fully optimized at the complete active space multiconfiguration self-consistent field level of theory[26−28] [CASSCF] in conjunction with the 6-31G(d) basis set.[29] The CASSCF wave function, labeled (9,6), was built up by distributing nine electrons in the six orbitals, which are most reasonably involved in the reaction mechanisms. With reference to the reactants, we included, in particular, the singly occupied *sp* hybrid orbitals of the Ge atom of the GeH_3 radicals and five orbitals of NF_3, namely, a pair of bonding and antibonding N−F sigma orbitals (σ_{N-F} and σ^*_{N-F}), two *p* orbitals of F, and the *n* orbital of N.

The geometries were also optimized with two different methods containing the electron correlation, the Møller−Plesset theory[30] with inclusion of inner electrons [MP2(full)], and the B3LYP[31] hybrid functional [B3LYP] with the 6-311G(d,p) basis set,[29] by gradient-based techniques[32−35] and with no symmetry constraints.

Any located critical point was unambiguously characterized as an energy minimum or a TS by calculating its analytical vibrational frequencies at all levels of theory. Any TS was also related to its interconnected energy minima by intrinsic reaction coordinate (IRC) calculations.[36] The unscaled frequencies were also used to calculate the zero-point vibrational energies (ZPE) and the vibrational contribution to the thermal correction (TC), obtained at 298.15 K by standard statistical mechanics formulas.[37] The overall TC term was finally obtained by adding the translational (3/2 RT) and rotational (RT or 3/2 RT) contributions at this temperature. Total entropies were also obtained by unscaled frequencies and moments of inertia. The absolute energies were refined by performing, at the CASSCF and MP(full) optimized geometries, single-point calculations with the CCSD(T,full)[38,39] method, using the 6-311++G(2d,2p) basis set.[29] The T1 diagnostics[40] were calculated at the same level of theory. Absolute energies were also calculated using the G3B3[41] composite methods on the B3LYP/ 6-311G(d,p) optimized geometries.

ASSOCIATED CONTENT

Supporting Information

The Supporting Information is available free of charge at https://pubs.acs.org/doi/10.1021/acsomega.9b03729.

Cartesian coordinates of all optimized geometries at the CASSCF/6-31G(d) level and the corresponding total energies at the CCSD(T,full)/6-311++G(2d,2p) level of theory (Table S1); cartesian coordinates of all optimized geometries at the B3LYP/6-311G(d,p) level and the corresponding total energies at the G3B3 level of calculation (Table S2); cartesian coordinates of all optimized geometries at the MP2(full)/6-311G(d,p) level and the corresponding total energies at the CCSD(T,full)/6-311++G(2d,2p) level of theory (Table S3); optimized geometries (Å and °) of complex **1′** formed before the transition states (Figure S1);

https://dx.doi.org/10.1021/acsomega.9b03729
ACS Omega 2020, 5, 4907−4914

relative energies, enthalpies, and free energies of the reactants and intermediate **1′** (Table S4) (PDF)

AUTHOR INFORMATION

Corresponding Author

Paola Antoniotti − *Dipartimento di Chimica, Università di Torino, 10125 Torino, Italy; CRISDI, Interdepartmental Centre for Crystallography, University of Turin, 10124 Torino, Italy;* orcid.org/0000-0003-2647-141X; Phone: +39-011-6707519; Email: paola.antoniotti@unito.it

Authors

Paola Benzi − *Dipartimento di Chimica, Università di Torino, 10125 Torino, Italy; CRISDI, Interdepartmental Centre for Crystallography, University of Turin, 10124 Torino, Italy;* orcid.org/0000-0001-7046-2022

Domenica Marabello − *Dipartimento di Chimica, Università di Torino, 10125 Torino, Italy; CRISDI, Interdepartmental Centre for Crystallography, University of Turin, 10124 Torino, Italy;* orcid.org/0000-0002-9648-7735

Daniele Rosso − *Dipartimento di Chimica, Università di Torino, 10125 Torino, Italy*

Complete contact information is available at: https://pubs.acs.org/10.1021/acsomega.9b03729

Notes

The authors declare no competing financial interest.

ACKNOWLEDGMENTS

The authors thank the Università di Torino and the Ministero Italiano dell'Istruzione, dell'Università e della Ricerca (MIUR) for financial support.

REFERENCES

(1) (a) Davies, G.; Roberts, B. P. In *Free Radicals*, Kochi, J. K., Ed.; Wiley: New York, 1973; Chapter 10, Vol. *1*. (b) Fossey, J.; Lefort, D.; Sorba, J. *Free Radicals in Organic Chemistry*; Wiley: Chichester, 1995; 123.

(2) (a) Schiesser, C. H.; Wild, L. M. Free-radical homolytic substitution: New methods for formation of bonds to heteroatoms. *Tetrahedron* **1996**, *42*, 13265−13314. (b) Schiesser, C. H.; Smart, B. A.; Tu-Anh, Tran. An ab initio study of some free-radical homolytic substitution reactions at halogen. *Tetrahedron* **1995**, *51*, 3327−3338.

(3) (a) Schiesser, C. H.; Smart, B. A. An ab initio study of some free-radical homolytic substitution reactions at sulfur, selenium and tellurium. *Tetrahedron* **1995**, *51*, 6051−6060. (b) Schiesser, C. H.; Smart, B. A. On the existence of SH_3, SeH_3, and TeH_3: Discrepancies between all-electron and pseudopotential calculations. *J. Comput. Chem.* **1995**, *16*, 1055−1066.

(4) (a) Horvat, S. M.; Schiesser, C. H. An ab initio and DFT study of homolytic substitution reactions of acyl radicals at sulfur, selenium, and tellurium. *New J. Chem.* **2010**, *34*, 1692−1699. (b) Schiesser, C. H.; Wild, L. M. Intramolecular Homolytic Substitution Chemistry: An ab Initio Study of 1,n-Chalcogenyl Group Transfer and Cyclization Reactions in Some ω-Chalcogenylalkyl Radicals. *J. Org. Chem.* **1999**, *64*, 1131−1139.

(5) (a) Schiesser, C. H.; Wild, L. M. Homolytic Substitution at Phosphorus: An Ab initio Study of the Reaction of Hydrogen Atom and Methyl Radical With Phosphine and Methylphosphine. *Aust. J. Chem.* **1995**, *48*, 175−184. (b) Cramer, C. J. Theoretical Rotation, Pseudorotation, and Pseudoinversion Barriers for the Hydroxyphosphoranyl Radical. *J. Am. Chem. Soc.* **1990**, *112*, 7965−7972. (c) Cramer, C. J. The fluorophosphoranyl f series: theoretical insights into relative stabilities and localization of spin. *J. Am. Chem. Soc.* **1991**, *113*, 2439−2447.

(6) (a) Matsubara, H.; Horvat, S. M.; Schiesser, C. H. Methyl radical also reacts by the frontside mechanism: An ab initio study of some homolytic substitution reactions of methyl radical at silicon, germanium and tin. *Org. Biomol. Chem.* **2003**, *1*, 1199−1203. (b) Matsubara, H.; Schiesser, C. H. An ab-initio study of some homolytic substitution reactions of acyl radicals at silicon, germanium and tin. *Org. Biomol. Chem.* **2003**, *1*, 4335−4341.

(7) Lucas, M.; Thomas, A. M.; Yang, T.; Kaiser, R. I.; Mabel, A. M.; Hait, D.; Head-Gordon, M. Bimolecular Reaction Dynamics in the Phenyl−Silane System: Exploring the Prototype of a Radical Substitution Mechanism. *J. Phys. Chem. Lett.* **2018**, *9*, 5135−5142.

(8) Horvat, S. M.; Schiesser, C. H.; Wild, L. M. Free Radical Homolytic Substitution by the Frontside Mechanism: Ab Initio Study of Homolytic Substitution Reactions at Silicon, Germanium, and Tin. *Organometallics* **2000**, *19*, 1239−1246.

(9) Cadman, P.; Inel, Y.; Trotman-Dickenson, A. F. Thermal reaction of $(CH_3)_2C{=}C(CH_3)_2$ in the presence of di-tert-butyl peroxide; reactions of the radicals $^{\cdot}CH_3$, $(CH_3)_3\dot{C}C(CH_3)_2$ and $(CH_3)_2C{=}C(CH_3)\dot{C}H_2$. *J. Chem. Soc., Faraday Trans. II* **1978**, *74*, 2301−2312.

(10) (a) Belter, R. K. High temperature vapor phase reactions of nitrogen trifluoride with benzylic substrates. *J. Fluorine Chem.* **2011**, *132*, 318−322. (b) Belter, R. K. Difluoroalkylamines from high temperature vapor phase reactions of nitrogen trifluoride with alkanes, ethers and benzene. *J. Fluorine Chem.* **2011**, *132*, 961−964. (c) Belter, R. K.; McFerrin, C. A. Ab initio study of the mechanisms of reactions of NF_3 with aliphatic and benzylic substrates. *J. Fluorine Chem.* **2012**, *135*, 272−277. (d) Belter, R. K. ^{19}F NMR of linear N, N-difluoroaminoalkanes. *J. Fluorine Chem.* **2012**, *137*, 73−76.

(11) Antoniotti, P.; Benzi, P.; Borocci, S.; Demaria, C.; Giordani, M.; Grandinetti, F.; Operti, L.; Rabezzana, R. Bimolecular homolytic substitutions at nitrogen: an experimental and theoretical study on the gas phase reactions of alkyl radicals with NF_3. *Chem. Eur. J.* **2015**, *21*, 15826−15834.

(12) (a) Antoniotti, P.; Operti, L.; Rabezzana, R.; Turco, F.; Vaglio, G. A. Gas-phase ion chemistry of Si^+ and NF_3: An experimental and theoretical study. *Int. J. Mass Spectrom.* **2006**, *255-256*, 225−231. (b) Antoniotti, P.; Rabezzana, R.; Turco, F.; Borocci, S.; Giordani, M.; Grandinetti, F. Ion chemistry in germane/fluorocompounds gaseousmixtures: a mass spectrometric and theoretical study. *J. Mass Spectrom.* **2008**, *43*, 1320−1333. (c) Antoniotti, P.; Operti, L.; Rabezzana, R.; Turco, F.; Zanzottera, C.; Giordani, M.; Grandinetti, F. Gas-phase reactions of XH_3^+ (X = C, Si, Ge) with NF_3: a Comparative Investigation on the Detailed Mechanistic Aspects. *J. Mass Spectrom.* **2009**, *44*, 1348−1358. (d) Antoniotti, P.; Operti, L.; Rabezzana, R.; Turco, F.; Borocci, S.; Grandinetti, F. Positive ion chemistry of SiH_4/NF_3 gaseous mixtures studied by ion trap mass spectrometry. *Eur. J. Mass Spectrom.* **2009**, *15*, 209−220. (e) Antoniotti, P.; Bottizzo, E.; Borocci, S.; Giordani, M.; Grandinetti, F. Gas-phase reactions of SiH_n^+ (n = 1,2) with NF_3: a computational investigation on the detailed mechanistic aspects. *J. Comput. Chem.* **2012**, *33*, 1918−1926.

(13) Spinks, J. W. T.; Wood, R. J. In *An Introduction to Radiation Chemistry*, 3rd ed.; John Wiley & Sons: New York, 1990; pp 3−13.

(14) Fraden, J. In *AIP Handbook of Modern Sensors, Physics, Designs, and Applications*, 4th ed; Springer Science + Business Media: New York, 2010; pp 508−509.

(15) (a) Antoniotti, P.; Benzi, P.; Castiglioni, M.; Volpe, P. An Experimental and Theoretical Study of Gaseous Products in the Radiolysis of Germane/Ethylene Mixtures. *Eur. J. Inorg. Chem.* **1999**, 323−327. (b) Newman, C. G.; Dzarnoski, J.; Ring, M. A.; O'Neal, H. E. Kinetics and mechanism of the germane decomposition. *Int. J. Chem. Kinet.* **1980**, *12*, 661−670.

(16) (a) Lias, S. G.; Bartmess, J. E.; Liebman, J. F.; Holmes, J. L.; Levin, R. D.; Mallard, W. G. Gas-phase ion and neutral thermochemistry. *J. Phys. Chem. Ref. Data Suppl. 1* **1988**, *17*, 1−861. (b) Cavallotti, C.; Polino, D.; Barbato, A. An Ab Initio RRKM/Master Equation Investigation of SiH_4 and GeH_4 Decomposition

Kinetics Using a Kinetic Monte Carlo Approach. *ECS Trans.* **2009**, *25*, 445−452.
(17) (a) Benzi, P.; Operti, L.; Vaglio, G. A.; Volpe, P.; Speranza, M.; Gabrielli, R. Gas phase ion-molecule reaction of monogermane with oxygen and ammonia. *J. Organomet. Chem.* **1988**, *354*, 39−50. (b) Antoniotti, P.; Benzi, P.; Castiglioni, M.; Operti, L.; Volpe, P. Radiolysis of binary systems containing germanium and carbon hydrides. *Radiat. Phys. Chem.* **1996**, *48*, 457−462.
(18) McMahon, T. B.; Heinis, T.; Nicol, G.; Hovey, J. K.; Kebarle, P. Methyl cation affinities. *J. Am. Chem. Soc.* **1988**, *110*, 7591−7598.
(19) Yakobson, V. V.; Musaev, D. G.; Zyubin, A. S.; Mebel, A. M.; Charkin, O. P. Theoretical study of Li^+ affinity of the hydrides MH_n, fluorides MF_n, and lithides MLi_n molecules. *Koord. Khim.* **1989**, *15*, 1478−1488.
(20) (a) Grandinetti, F.; Hrušàk, J.; Schröder, D.; Karrass, S.; Schwarz, H. Nitrogen versus fluorine protonation of nitrogen fluoride in the gas-phase. A combined mass spectrometric and Gaussian-1 ab initio MO study reveals the the Existence of Two Distinct Isomers F_3NH^+ and F_2N-FH^+. *J. Am. Chem. Soc.* **1992**, *114*, 2806−2810. (b) Grandinetti, F.; Cecchi, P.; Vinciguerra, V. Methylated NF_3. A G2MS theoretical study on the structure, stability, and interconversion of the CH_3−NF_3^+ and CH_3F−NF_2^+ isomers. *Chem. Phys. Lett.* **1997**, *281*, 431−437. (c) Grandinetti, F.; Vinciguerra, V. Complexes of lithium cation with nitrogen trifluoride: a computational investigation on the structure and stability of Li^+−(NF_3) isomers. *J. Mol. Struct.: Theochem* **2001**, *574*, 185−193. (d) Grandinetti, F.; Vinciguerra, V. Adducts of NF_2^+ with diatomic and simple polyatomic ligands: a computational investigation on the structure, stability, and thermochemistry. *Int. J. Mass Spectrom.* **2002**, *216*, 285−299. (e) Giordani, M.; Grandinetti, F. Protonated MF_3 (M = N−Bi): Structure, stability, and thermochemistry of the H−MF_3^+ and HF−MF_2^+ isomers. *J. Fluorine Chem.* **2009**, *130*, 557−561.
(21) Hiraoka, K.; Nasu, M.; Fujimaki, S.; Yamabe, S. Gas-Phase Positive-and Negative-Ion-Molecule Reactions in NF_3. *J. Phys. Chem. A* **1995**, *99*, 15822−15829.
(22) Duchowicz, P. R.; Cobos, C. J. Gaussian-3 study of the thermochemistry of the germane and its fluoro chloro derivatives. *J. Phys. Chem. A* **2008**, *112*, 6198−6204.
(23) Bronic, Krajcar. W values and Fano factors for electrons in rare gases and rare gas mixtures. *Hoshasen* **1998**, *24*, 101−125.
(24) Ruscic, B.; Schwarz, M.; Berkowitz, J. Photoionization studies of GeH_n (n = 2−4). *J. Chem. Phys.* **1990**, *92*, 1865−1875.
(25) Frisch, M. J.; Trucks, G. W.; Schlegel, H. B.; Scuseria, G. E.; Robb, M. A.; Cheeseman, J. R.; Scalmani, G.; Barone, V.; Mennucci, B.; Petersson, G. A.; Nakatsuji, H.; Caricato, M.; Li, X.; Hratchian, H. P.; Izmaylov, A. F.; Bloino, J.; Zheng, G.; Sonnenberg, J. L.; Hada, M.; Ehara, M.; M. Toyota, K.; Fukuda, R.; Hasegawa, J.; Ishida, M.; Nakajima, T.; Honda, Y.; Kitao, O.; Nakai, H.; Vreven, T.; Montgomery, J. A., Jr.; Peralta, J. E.; Ogliaro, F.; Bearpark, M.; Heyd, J. J.; Brothers, E.; Kudin, K. N.; Staroverov, V. N.; Kobayashi, R.; Normand, J.; Raghavachari, K.; Rendell, A.; Burant, J. C.; Iyengar, S. S.; Tomasi, J.; Cossi, M.; Rega, N.; Millam, J. M.; Klene, M.; Knox, J. E.; Cross, J. B.; Bakken, V.; Adamo, C.; Jaramillo, J.; Gomperts, R.; Stratmann, R. E.; Yazyev, O.; Austin, A. J.; Cammi, R.; Pomelli, C.; Ochterski, J. W.; Martin, R. L.; Morokuma, K.; Zakrzewski, V. G.; Voth, G. A.; Salvador, P.; Dannenberg, J. J.; Dapprich, S.; Daniels, A. D.; Farkas, Ö.; Foresman, J. B.; Ortiz, J. V.; Cioslowski, J.; Fox, D. J.. *Gaussian 09*, revision A.02; Gaussian, Inc.: Wallingford CT, 2009.
(26) Roos, B. O. In *Advances in Chemical Physics: Ab Initio Methods in Quantum Chemistry-II*, Lawley, K. P., Ed.; Wiley: New York, 1987, pp.399−445.
(27) Hegarty, D.; Robb, M. A. Application of unitary group-methods to configuration-interaction calculations. *Mol. Phys.* **1979**, *38*, 1795−1812.
(28) Robb, M. A.; Eade, R. H. A. In *Computational Theoretical Organic Chemistry*, Csizmadia, I. G.; Daudel, R., Eds.; Reidel Publ Co: Holland, 1981; pp 21−54.
(29) Hehre, W. J.; Radom, L.; Schleyer, P. V. R.; Pople, J. A. *Ab initio Molecular Orbital Theory*; Wiley: New York, 1986; 80.
(30) Møller, C.; Plesset, M. S. Note on an approximation treatment for many-electron systems. *Phys. Rev.* **1934**, *46*, 618−622.
(31) (a) Becke, A. D. Density-functional thermochemistry. III. The role of exact exchange. *J. Chem. Phys.* **1993**, *98*, 5648−5652. (b) Lee, C.; Yang, W.; Parr, R. G. Development of the Colle-Salvetti correlation-energy formula into a functional of the electron density. *Phys. Rev. B* **1988**, *37*, 785−789.
(32) Schlegel, H. B. In *Computational Theoretical Organic Chemistry*, Csizmadia, I. G.; Daudel, R., Eds.; Reidel Publ Co: Holland, 1981; pp 129−159.
(33) Schlegel, H. B. An efficient algorithm for calculating ab initio energy gradients using s, p Cartesian Gaussians. *J. Chem. Phys.* **1982**, *77*, 3676−3681.
(34) Schlegel, H. B.; Binkley, J. S.; Pople, J. A. First and second derivatives of two electron integrals over Cartesian Gaussians using Rys polynomials. *J. Chem. Phys.* **1984**, *80*, 1976−1981.
(35) Schlegel, H. B. Optimization of equilibrium geometries and transition structures. *J. Comput. Chem.* **1982**, *3*, 214−218.
(36) (a) Hratchian, H. P.; Schlegel, H. B. Accurate reaction paths using a Hessian based predictor−corrector integrator. *J. Chem. Phys.* **2004**, *120*, 9918−9924. (b) Hratchian, H. P.; Schlegel, H. B. in *Theory and Applications of Computational Chemistry: The First 40 Years*, Dykstra, C. E.; Frenking, G.; Kim, K. S.; Scuseria, G., Eds.; Elsevier: Amsterdam, 2005; pp 195−249. (c) Hratchian, H. P.; Schlegel, H. B. Using Hessian updating to increase the efficiency of a Hessian based predictor-corrector reaction path following method. *J. Chem. Theory Comput.* **2005**, *1*, 61−69.
(37) Mc Quarry, A. *Statistical Mechanics*, Harper & Row: New York, 1976.
(38) Raghavachari, K.; Trucks, G. W.; Pople, J. A.; Head-Gordon, M. A fifth-order perturbation comparison of electron correlation theories. *Chem. Phys. Lett.* **1989**, *157*, 479−483.
(39) Hampel, C.; Peterson, K.; Werner, H. J. A comparison of the efficiency and accuracy of the quadratic configuration interaction (QCISD), coupled cluster (CCSD), and Brueckner coupled cluster (BCCD) methods. *Chem. Phys. Lett.* **1992**, *190*, 1−12.
(40) Lee, T. J.; Taylor, P. R. A diagnostic for determining the quality of single-reference electron correlation methods. *Int. J. Quantum Chem.* **1989**, *36*, 199−207.
(41) Baboul, A. G.; Curtiss, L. A.; Redfern, P. C.; Raghavachari, K. Gaussian-3 theory using density functional geometries and zero-point energies. *J. Chem. Phys.* **1999**, *110*, 7650−7657.

https://dx.doi.org/10.1021/acsomega.9b03729
ACS Omega 2020, 5, 4907−4914